

## Ordered Nanoporous Silica with Periodic 30–60 nm Pores as an Effective Support for Gold Nanoparticle Catalysts with Enhanced Lifetime

Guicen Ma, Xiaoqing Yan, Yunlong Li, Liping Xiao, Zhangjun Huang, Yanping Lu, and Jie Fan\*

Key Lab of Applied Chemistry of Zhejiang Province, Department of Chemistry, Zhejiang University, Hangzhou, Zhejiang Province 310027, China

Received April 1, 2010; E-mail: jfan@zju.edu.cn

**Abstract:** We demonstrate that supermolecular templating allows tuning the pore size of ordered mesoporous materials in the once elusive range from 30 nm to more than 60 nm through simple control of synthetic variables (salt/supermolecule concentration and hydrothermal temperature). Gold nanoparticles (AuNPs) within the extra-large pores exhibit dramatically increased lifetime compared to those located within relatively small mesopores due to the enhanced mass diffusion that suppresses coke deposition on AuNPs.

Ordered mesoporous/nanoporous materials (OMMs) have great potential for applications in nanocatalysis, biological reactions, molecular sieves, drug delivery, and optoelectronics.<sup>1</sup> Precise tuning of their pore size distribution is critical to perform the desirable function of OMMs in a particular application. Variation of synthesis temperature and use of large-molecular-weight polymer templates have extended their pore size up to 30 nm.<sup>2</sup> However, the preparation of OMMs with pore size larger than 30 nm generally relies on the use of external, physical molds (e.g., polystyrene spheres, silica colloidal, and porous alumina membranes) because of dimensional limitations of supermolecular templates.<sup>3</sup> So far, the realization of OMMs with periodic 30–50 nm pores from supermolecular templates is a unfilled gap between the largest ordered mesoporous materials and the smallest ordered macroporous materials,<sup>1</sup> representing a significant synthetic challenge. Moreover, the extra-large mesopores (30–50 nm) would have immediate interest for certain fundamental problems, such as diffusion and phase equilibrium in restricted nanoscopic geometries. Catalysis and large-molecule separation processes would also benefit from more uniform and open porous networks that provide optimal mass diffusion and improved efficiency.<sup>3</sup>

Here, we report that the pore size range of OMMs from supermolecular templates can be extended into the very large pore regime (30–60 nm). Gold nanoparticles (AuNPs) within the extra-large pores exhibit dramatically increased lifetimes compared to those located within relatively small mesopores due to the enhanced mass diffusion.

The OMMs with extra-large mesopores (denoted as EP-FDU-12) are synthesized by using a common block copolymer (F127) as the template with the assistance of 1,3,5-trimethylbenzene (TMB) and an inorganic salt (KCl). The procedure is similar to that for LP-FDU-12,<sup>2a</sup> except that the concentrations of F127 and KCl are significantly reduced (see Supporting Information (SI)). EP-FDU-12 shows excellent FDU-12-type face-centered-cubic (fcc) mesostructures with a very large cell parameter of 50.5 nm, as confirmed by small-angle X-ray scattering (SAXS) and transmission electron microscopy (TEM) analyses (Figure 1). The highly ordered three-dimensional mesostructure is also reflected in their crystal-like hexagonal-prism morphology (Figure 1b,c). High-resolution SEM images show that hexagonal arrays of uniform cages (~33.5 nm) are found throughout the top and side faces of the hexagonal prisms, indicating that both the top and side faces of

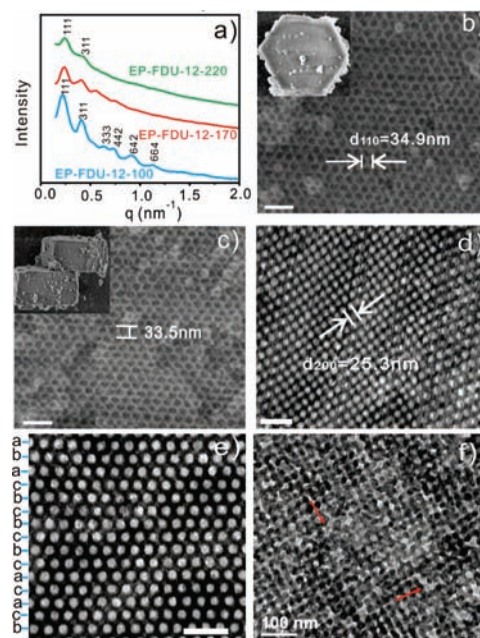


**Figure 1.** (a) SAXS patterns of EP-FDU-12 samples. (b,c) SEM images of EP-FDU-12-100, (b) top and (c) side views. (d–f) TEM images of microtomed EP-FDU-12-100 viewed along the (d) [100] and (e) [110] directions and (f) of EP-FDU-12-220 viewed along the [100] direction. All scale bars are 100 nm.

the hexagonal prisms are enclosed by {1,1,1} facets. The cell parameter calculated from the SEM images is 50 nm, in good agreement with the SAXS and TEM results. It is worth noting that there is no intrinsic driving force for EP-FDU-12 to grow into two-dimensional crystals since its fcc structure has a cubic symmetry. This observation suggests that a multiple parallel twin planar defect is involved in the early stage of the crystal growth of fcc mesostructures, as confirmed by TEM analysis (Figure 1e),<sup>4</sup> which is also found in other fcc structured OMMs.<sup>5</sup>

Figure 2 shows the nitrogen sorption isotherm of EP-FDU-12-100 (-100 indicating hydrothermal treatment temperature), which is a type IV nitrogen sorption isotherm with a broad, intermediate hysteresis loop between H1 and H2. The pore size of EP-FDU-12-100 is calculated to be 31.6 nm on the basis of a modified BdB model (close to SEM observation),<sup>6</sup> which is about 50% larger than that of LP-FDU-12 (22 nm) prepared at same synthesis and hydrothermal-treatment temperatures. The pore size of EP-FDU-12 can be further expanded up to 62 nm by increasing the hydrothermal-treatment temperature from 100 to 220 °C (Figure 2a). After such a high-temperature hydrothermal treatment, the ordered fcc structure of EP-FDU-12 is maintained. The cell parameter of EP-FDU-12-220 is the same as that for EP-FDU-12-100 (Figure 1a, SI). TEM and nitrogen sorption studies reveal that the ultra-large nanopores of EP-FDU-12-220 are interconnected by randomly distributed extra-large windows

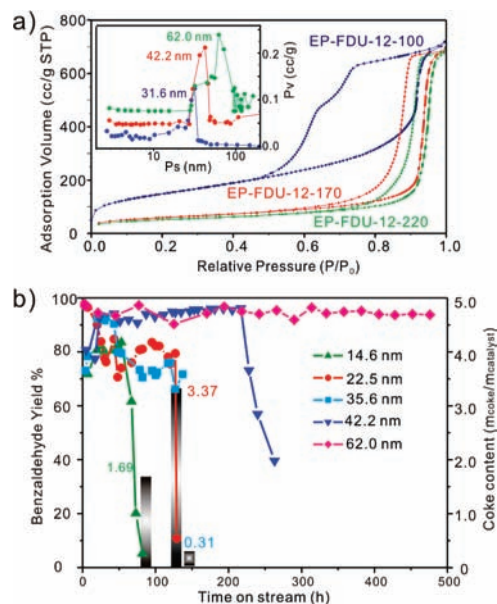


**Figure 2.** (a) Nitrogen sorption isotherms and pore size distribution plots of mesoporous silica EP-FDU-12. (b) Time-on-stream benzaldehyde yields and coke contents over AuNPs/OMMs catalysts with different pore sizes.

(34.8 nm) formed after high-temperature hydrothermal treatment (indicated by red arrows). To our knowledge, these are the first supermolecular-templated OMMs that bridge the gap between the largest ordered mesoporous silica and small macroporous silica.

In comparison with LP-FDU-12 synthesis, the significantly reduced KCl and F127 concentration in EP-FDU-12 synthesis is believed to be responsible for the unprecedented pore expansion. In the synthesis of LP-FDU-12, it was speculated that a micelle-to-unimer transition induced by low temperature is crucial for TMB penetration into the hydrophobic PPO core of PEO-PPO-PEO micelles and subsequent pore expansion.<sup>2a</sup> In this study, we applied dynamic light scattering (DLS) to monitor the micellization behavior of F127 at different temperatures and compared it with temperature-dependent pore size variation (SI). It is found that the micelle-to-unimer transition occurs in the temperature range of 20–23 °C. No obvious pore size variation is observed in the micelle temperature region (>23 °C), while significant pore expansion occurs in the unimer temperature region (<20 °C). At a lower KCl concentration, a similar behavior is observed, with the pore expansion only occurring in the unimer temperature region (<25 °C). These results argue the proposed TMB penetration model in LP-FDU-12 synthesis, in which efficient TMB swelling is required to break the micelle structures, which serves as a guide to explore new synthetic strategies for more efficient TMB swelling and subsequent pore size expansion.

The effect of salt and surfactant concentration on the micellization has been well documented.<sup>7</sup> DLS experiments reveal that reducing the KCl/F127 concentration leads to the structure-breaking of F127 micelles and the formation of the unimers. Thus, the reduced KCl/F127 concentration in EP-FDU-12 synthesis could be regarded as an extension of the previous low-temperature strategy that leads to more efficient TMB swelling and subsequent pore expansion.

Catalysis processes could benefit from the three-dimensional extra-large mesoporous networks of EP-FDU-12 that provide optimal mass diffusion. Many industrial catalysts used today are metal nanoparticles that are spread over the internal surface of porous materials, acting as carriers or supports. The catalytic performance of mesoporous silica EP-FDU-12 as the support for AuNPs is compared to that of OMMs with smaller mesopores in gas-phase benzyl alcohol selective oxidation

using molecular oxygen as the oxidant. Five AuNPs/OMMs (0.5 wt %) catalysts with different pore sizes (15, 23, 36, 42, and 62 nm) were prepared by direct deposition of AuNPs onto the OMMs in chloroform solution (SI). There is no significant initial activity difference among the five AuNPs/OMMs catalysts. They are all highly selective in benzyl alcohol-to-benzaldehyde transformation (selectivity >99%) (Figure 2b). In spite of their initial high conversion, the activity of AuNPs supported on the OMMs with the smallest mesopores (15 nm) rapidly decreases after 60 h of reaction (TON  $\approx$  302 000). The sharp loss of catalytic activity can probably be ascribed to the formation of pitch-dark deposits on the catalyst.<sup>8</sup> With time-on-stream, however, the AuNPs/EP-FDU-12 catalysts deactivate far more slowly than other two AuNPs/OMMs catalysts with smaller mesopores. TEM studies confirm that the particle size of AuNPs supported on EP-FDU-12-140 (36 nm) is similar to those on OMMs (23 nm) ( $11.3 \pm 2.7$  nm vs  $10.3 \pm 2.7$  nm) (SI). Only 12% Au leaching is confirmed by ICP analysis for the deactivated catalyst, indicating that AuNPs leaching is not the main reason for the activity loss. However, thermal gravimetric analysis reveals that there is at least 10-fold less carbon deposition on AuNPs/EP-FDU-12-140 (36 nm) than on AuNPs/OMMs (23 nm) (0.31 vs 3.37,  $m_{\text{coke}}/m_{\text{catalyst}}$ ), suggesting that large and opened three-dimensional mesoporous networks facilitate the rapid diffusion of organic products out of reaction zones and thus suppress coke formation. After a continuous 450 h reaction, there is no activity decrease for AuNPs supported on EP-FDU-12-220 (62 nm). The turnover number accounts to 3 070 000, a notably higher number as compared with typical supported Au catalysts.<sup>8</sup>

To conclude, we demonstrated that supermolecular templating allows tuning of the pore size of OMMs in the once elusive range from 30 nm to more than 60 nm through simple control of synthetic variables (salt/F127 concentration and hydrothermal temperature). The pore size variation is important not only for the design of better porous catalysts but also for other applications (like large molecular separation and hosting of quantum size objects) that could also benefit from the fine control of mesopore size.

**Acknowledgment.** We are grateful for financial support from the National Science Foundation of China (20873122 and J0830413), Science & Technology Department of Zhejiang Province (2008C11125), and the Fundamental Research Funds for the Central Universities (2009QNA3005). This work made use of the SAXS facility in the Laboratory of Advanced Materials at Fudan University.

**Supporting Information Available:** Synthesis and characterization of mesoporous materials. This material is available free of charge via the Internet at <http://pubs.acs.org>.

## References

- (1) (a) Wan, Y.; Zhao, D. Y. *Chem. Rev.* **2007**, *107*, 2821–2860. (b) Stein, A.; Schrodin, R. C. *Curr. Opin. Solid State Mater. Sci.* **2001**, *5*, 553–564. (c) Hartmann, M. *Chem. Mater.* **2005**, *17*, 4577–4593.
- (2) (a) Fan, J.; Yu, C. Z.; Lei, J.; Zhang, Q.; Li, T. C.; Tu, B.; Zhou, W. Z.; Zhao, D. Y. *J. Am. Chem. Soc.* **2005**, *127*, 10794–10795. (b) Deng, Y. H.; Yu, T.; Wan, Y.; Shi, Y. F.; Meng, Y.; Gu, D.; Zhang, L. J.; Huang, Y.; Liu, C.; Wu, X. J.; Zhao, D. Y. *J. Am. Chem. Soc.* **2007**, *129*, 1690–1697. (c) Yu, K.; Hurd, A. J.; Eisenberg, A.; Brinker, C. J. *Langmuir* **2001**, *17*, 7961–7965.
- (3) (a) Holland, B. T.; Blanford, C. F.; Stein, A. *Science* **1998**, *281*, 538–540. (b) Johnson, S. A.; Ollivier, P. J.; Mallouk, T. E. *Science* **1999**, *283*, 963–965. (c) Yang, Z.; Lu, Y. *Angew. Chem., Int. Ed.* **2003**, *42*, 4719–4719.
- (4) Sakamoto, Y.; Diaz, I.; Terasaki, O.; Zhao, D. Y.; Perez-Pariente, J.; Kim, J. M.; Stucky, G. D. *J. Phys. Chem. B* **2002**, *106*, 3118–3123.
- (5) Sakamoto, Y.; Han, L.; Che, S. N.; Terasaki, O. *Chem. Mater.* **2009**, *21*, 223–229.
- (6) Lukens, W. W.; Schmidt-Winkel, P.; Zhao, D. Y.; Feng, J. L.; Stucky, G. D. *Langmuir* **1999**, *15*, 5403–5409.
- (7) Desai, P. R.; Jain, N. J.; Sharma, R. K.; Bahadur, P. *Colloids Surf. A—Physicochem. Eng. Asp.* **2001**, *178*, 57–69.
- (8) Pina, C. D.; Falletta, E.; Rossi, M. J. *Catal.* **2008**, *260*, 384–396.

JA1027524